

# Bi-azimuthally symmetric solutions of $d = 4 + 1$ Einstein-Yang-Mills $SU(2)$ theory

Eugen Radu<sup>a</sup>, Ya. M. Shnir<sup>b\*</sup> and D. H. Tchrakian<sup>c</sup>

<sup>a</sup>*University of Tours, CNRS, France*

<sup>b</sup>*School of Mathematics, TCD, Ireland*

<sup>c</sup>*Department of Mathematical Physics. NUI Maynooth, Ireland*

## Abstract

We construct static, asymptotically flat solutions of  $SU(2)$  Einstein-Yang-Mills theory in  $4 + 1$  dimensions, subject to bi-azimuthal symmetry. The results are compared with similar solutions of the  $SU(2)$  Yang-Mills-dilaton model. Both particle-like and black hole solutions are considered for two different sets of boundary conditions in the Yang-Mills sector, corresponding to multisolitons and soliton-antisoliton pairs. For gravitating multi-soliton solutions, we find that their mass per unit charge is lower than the mass of the corresponding unit charge, spherically symmetric soliton.

The last years have seen an increasing interest in the solutions of Einstein equations involving more than four dimensions. The results in the literature indicate that the physics in higher-dimensional general relativity is far richer and complex than in the standard four-dimensional theory.

Naturally, most of the studies in the literature were carried out for vacuum solutions or to configurations with an Abelian matter content. At the same time, a number of results in the literature clearly indicate that solutions to the Einstein equations coupled to non Abelian matter fields possess a much richer structure than in the  $U(1)$  case (see [1] for a survey of the situation in four dimensions and the more recent review [2] for  $d > 4$ ), most notably in that they are not restricted to black holes, but can also be regular.

Physically reasonable stationary vacuum solutions in higher dimensional spacetimes,  $d \geq 4$ , fall in two categories, distinguished by their asymptotic behaviours. In the first category, there are the static spherically symmetric solutions generalising the  $d = 4$  Schwarzschild black hole, found by Tangherlini a long time ago [3], the rotating Myers-Perry solution [4] generalising the four dimensional Kerr black hole, and more recently the black ring solutions [5, 6]. In all these cases, the  $d$ -dimensional spacetime approaches asymptotically the  $\mathcal{M}^d$  Minkowski background. The second category are the black string solutions, and the corresponding black  $p$ -branes generalizations [7]. The black strings approach asymptotically  $d - 1$  dimensional Minkowski-spacetime times a circle,  $\mathcal{M}^{d-1} \times S^1$ , and in the simplest case present translational symmetry along the extra-coordinate direction. (Such configurations are important if one supposes the existence of extra dimensions in the universe, which are likely to be compact and described by a Kaluza-Klein (KK) theory.)

As is the case with the usual Schwarzschild black hole, all these vacuum solutions can be extended to describe configurations with an Abelian matter content. The inclusion of non Abelian matter fields is less systematic and is complicated by the fact that all known such solutions can only be evaluated numerically, starting from the earliest found Einstein-Yang-Mills (EYM) solution in four spacetime dimensions discovered by Bartnik and McKinnon [8].

---

\*e-mail: shnir@maths.tcd.ie

Spherically symmetric solutions to EYM systems in  $d$ -spacetime dimensions, approaching asymptotically the  $\mathcal{M}^d$  Minkowski background, were constructed systematically in [9]-[15]. The Yang–Mills (YM) sector of the systems studied there consisted of all needed terms belonging to the YM hierarchy [16, 17], which are higher order in the YM curvature in the manner of the Skyrme model. Such terms may arise in the low energy effective action of string theory [18, 19, 20]. It has been established that only in the presence of these higher order in the YM curvature terms, does the EYM solution lead to a finite mass. In the absence of such Skyrme-like terms, for example in [21, 22] (in  $d = 5$ ), the mass of the solution diverges. Both particle like and black hole solutions were constructed. The properties of these configurations are rather different from the familiar Bartnik-McKinnon solutions [8] in  $d = 4$ , and are somewhat more akin to the gravitating monopole solutions to EYM-Higgs system [23], which is not surprising since the latter features the dimensionful vacuum expectation value (VEV) of the Higgs field, while the former contain additional dimensionful terms entering as the couplings of the higher order YM terms.

As for solutions to the EYM system in  $d$  dimensional spacetime whose vacuum has the structure of  $\mathcal{M}^{d-1} \times S^1$  like the black string solutions, these are only constructed if one of the spacelike dimensions is supposed to be compact, and a Kaluza-Klein descent is performed, essentially eliminating that coordinate. Such solutions are given for  $d = 5$  in [21]-[27]. However, in the present work we will not be concerned with this type of solutions.

Our aim in the present work is to extend the construction of asymptotically flat finite mass EYM solutions vacuum, relaxing the constraint of spherical symmetry in the  $d - 1$  dimensional spacelike subspace as in [9]-[15].

The simplest possibility is to consider the imposition of a symmetry which leads to two a dimensional reduced effective system, rather than the one dimensional one in the previous examples. This is the first such attempt in the literature, and the numerical work of solving a two dimensional EYM boundary value problem is a task of considerable complexity. To achieve a two dimensional subsystem, we have found that the simplest option is to impose bi-azimuthal symmetry on the  $d = 5$  static EYM system. This is why we have restricted to  $d = 5$ , for otherwise a similar application of azimuthal symmetries in each plane would result in multi-azimuthal <sup>1</sup> subsystems, with higher dimensional boundary value problems to be solved, technically beyond the scope of this work.

As a warmup for the task at hand, we carry out the same program with the dilaton replacing gravity. The results then are compared with the counterpart solutions of the  $d = 4 + 1$  static EYM system with bi-azimuthal symmetry. Note that in this case also higher order gauge curvature terms are included in the action to enable the existence of finite mass solutions.

While we have restricted to five dimensional EYM solutions for technical reasons, this example is of considerable physical relevance since it enters all  $d = 5$  gauged supergravities as the basic building block and one can expect the basic features of its solutions to be generic. Also special about  $d = 5$  gravitating YM is the particular critical properties of the solutions present in all  $d = 4p + 1$  analysed in [12], and first discovered in [10]. Indeed in the  $d = 5$  YM-dilaton (YMd) system, studied in [29], these critical properties were present, providing yet another confirmation that dilaton interactions with YM, mimic [30] those with Einstein gravity.

The purpose of this paper is to present numerical arguments for the existence of a class of static  $d = 5$  solutions to the EYM equations of the model studied in [10], but now, subject to bi-azimuthal symmetry. These configurations present a spacetime symmetry group  $R \times U(1) \times U(1)$ , where  $R$  denotes time translation symmetry and the  $U(1)$  factors the rotation symmetry in two

---

<sup>1</sup>If one applied instead, spherical symmetry in the  $d - 2$  dimensional subspace of the  $d - 1$  spacelike dimensions, then the residual subsystems will always be *two dimensional* irrespective of the value of  $d$ . For example in  $d = 5$  this would be the  $SO(3)$  symmetry in the 3 dimensional subspace of the 4 spacelike dimensions, exactly as for the axially symmetric instantons [28]. While this may appear to be an attractive alternative, we have found that tackling the boundary value problem in that case is a considerably harder task, even in  $d = 4$ .

orthogonal planes. We present both regular and black hole solutions. In the particle like case we find solutions with many similar properties to those of the four dimensional  $SU(2)$  YM multi-instantons and composite instanton-antiinstanton bound states with  $U(1) \times U(1)$  symmetry, reported in Ref. [31].

## 1 $d = 4 + 1$ Yang–Mills-dilaton model

A particular feature of the model to be introduced in the next section is that it features a term that is higher order in the YM curvature. As will be explained in section 2, such terms are necessary to ensure that the solution yields a finite mass. Such terms were employed in previous works [9, 10, 12, 13, 15, 14] with precisely the same purpose. The physical justification for introducing higher order YM terms, which goes hand in hand with the inclusion of higher order gravitational terms, is that these occur in the low energy effective action of string theory [41]. Thus in principle the choice of higher dimensional EYM models involves the selection of higher order terms in the gravitational and non Abelian curvatures, namely the Riemann and the YM curvatures, which are reparametrisation and gauge invariant. Because we are concerned with finding classical solutions, we impose a pragmatic but important further restriction, namely that we consider only those Lagrange densities that are constructed from antisymmetrised  $2p$  curvature forms, and exclude all other powers of both Riemann and YM curvature 2-forms. (In the gravitational case this results in the familiar Gauss–Bonnet type Lagrangians, while in the case of non Abelian matter to the YM hierarchy pointed out in footnote 3 below.) As a result, only *velocity-squared* fields appear in the Lagrangian, which is what is needed both for physical reasons and for solving the classical field equations. In practice we add only the minimal number of such higher order terms that are necessitated by the requirements of finite mass. This criterion makes the inclusion of higher order gravitational terms unnecessary since we know from the (numerical) results of [9] that the qualitative properties of the classical solutions are insensitive to them. In addition to this argument based on numerical results there is an independent argument advanced at the end of section 2 of [13], based on the symmetries of the (higher order) gravitational terms, which in the absence of a dilaton dispenses with the effectiveness of employing such terms. This leaves one with higher order YM curvature terms only, whose status in the context of the string theory effective action is complex and as yet not fully resolved. While YM terms up to  $F^4$  arise from (the non Abelian version of) the Born–Infeld action [18], it appears that this approach does not yield all the  $F^6$  terms [19]. Terms of order  $F^6$  and higher can also be obtained by employing the constraints of (maximal) supersymmetry [42]. The results of the various approaches are not identical. In this background, we restrict our considerations to terms in the YM hierarchy (see footnote 3) only, in particular to the first two terms.

Concerning our particular choice of  $4 + 1$  spacetime dimensions here, our reasons are: When imposing axial symmetry on a YM field in  $d = D + 1$  dimensions the simplest way is, following [28], to impose spherical symmetry in the  $D - 1$  dimensional subspace of the  $d$  spacelike dimensions. In this case the Chern–Pontryagin topological charge is fixed by the boundary conditions imposed on the first polar angle, and no analogue of the vortex number appearing in the axially symmetric Ansatz for  $d = 3$  [43] is featured [28]. Technically, the absence of a vortex number makes the numerical integration much harder. Imposing axial symmetry in turns in the  $x - y$  and  $z - u$  planes of  $D = 4$  Euclidean space as in [31] on the other hand, features two (equal) vortex numbers, making the numerical work technically more accessible. It is our intention to use the particular bi-azimuthally symmetric Ansatz of [31] in  $D = 4$  that has led us to restrict ourselves to  $d = 4 + 1$  dimensional spacetime. (Numerical work on implementing axial symmetry like in [28] is at present in active progress.) Of course, the exploitation of this type of symmetry is not restricted to  $4 + 1$  spacetime, but can be extended to any odd  $2q + 1$  spacetime where  $q$  distinct azimuthal symmetries are imposed, but this in practice results in residual PDE’s of

order three and higher for  $q \geq 3$ .

## 1.1 The ansatz and field equations

The model in 5 spacetime dimensions with coordinates  $x_M = (x_0, x_\mu)$  that we study here is described by the Lagrangian

$$\mathcal{L}_m = \frac{1}{4\pi^2} \left( |\partial_M \phi|^2 + \left( \frac{\tau_1}{2 \cdot 2!} e^{2a\phi} \text{Tr} \mathcal{F}_{MN}^2 + \frac{\tau_2}{2 \cdot 4!} e^{6a\phi} \text{Tr} \mathcal{F}_{MNR S}^2 \right) \right) \quad (1)$$

where  $\phi$  is the dilaton field,  $\mathcal{F}_{MN} = \partial_M \mathcal{A}_N - \partial_N \mathcal{A}_M + [\mathcal{A}_M, \mathcal{A}_N]$  is the 2-form YM curvature and  $\mathcal{F}_{MNR S} = \{\mathcal{F}_{M[N, \mathcal{F}_{RS}]}\}$  is the 4-form YM curvature consisting of the totally antisymmetrised product of two YM 2-form YM curvatures (here the bracket  $[\nu\rho\sigma]$  implies cyclic symmetry) and  $\tau_1, \tau_2$  are dimensionful coupling strengths.

Let us give a brief justification for the choice of the model (1). The YM system, which scales as  $L^{-4}$ , in  $d = 4 + 1$  supports static solitons, namely the BPST instantons in  $d = 4 + 0$  dimensions. When the usual Einstein–Hilbert gravity, which scales as  $L^{-2}$ , is added to the YM term, the soliton collapses because of the (Derrick) scaling mismatch. To compensate for this mismatch a term scaling as  $L^{-\nu}$ , with  $\nu \geq 5$  must be added. If one is to restrict to positive definite terms<sup>2</sup>,  $\nu$  will be even, and the most economical choice is  $\nu = 6$ . A typical such term would be  $\text{Tr} (F \wedge DX)^2$ , where  $X$  is a scalar field, *e.g.* a Higgs or sigma–model field. This necessitates the introduction of a completely new (scalar) field which unlike the dilaton is not directly recognised as a constituent of a low energy effective action. For this reason we eschew this choice, and restrict our attention instead to systems featuring only YM (and eventually YMd) fields. The most economical choice then is to compensate with the YM term  $\text{Tr} (F \wedge F)^2$ , scaling with  $\nu = 4$ . We note, finally, that adding a (positive or negative) cosmological constant does not remedy the scaling mismatch since these terms do not scale at all.

The YM and dilaton field equations read

$$\tau_1 D_\mu \left( e^{2a\phi} \mathcal{F}^{\mu\nu} \right) + \frac{1}{2} \tau_2 \{ \mathcal{F}_{\rho\sigma}, D_\mu \left( e^{6a\phi} \mathcal{F}^{\mu\nu\rho\sigma} \right) \} = 0, \quad (2)$$

$$\nabla^2 \phi = \frac{a}{2\pi^2} \left( 2e^{2a\phi} \hat{L}_1 + 6e^{6a\phi} \hat{L}_2 \right). \quad (3)$$

In (3) we have used the notation

$$\hat{L}_1 = \frac{\tau_1}{2 \cdot 2!} \text{Tr} \mathcal{F}_{MN}^2, \quad \hat{L}_2 = \frac{\tau_2}{2 \cdot 4!} \text{Tr} \mathcal{F}_{MNR S}^2. \quad (4)$$

The construction of a YM Ansatz compatible with the symmetries of the above line element has been discussed at length in [29], [31]. We consider a  $d = 5$  static metric form with two orthogonal commuting rotational Killing vectors

$$ds^2 = -f(r, \theta) dt^2 + \frac{s(r, \theta)}{f(r, \theta)} (dr^2 + r^2 d\theta^2) + \frac{l(r, \theta)}{f(r, \theta)} r^2 \sin^2 \theta d\varphi^2 + \frac{p(r, \theta)}{f(r, \theta)} r^2 \cos^2 \theta d\psi^2, \quad (5)$$

where  $r$  is the radial coordinate, and  $\theta, \varphi, \psi$  are Hopf coordinates in  $S^3$ , with  $0 \leq \theta \leq \pi/2$  and  $0 \leq \varphi, \psi \leq 2\pi$ . Evidently, in the flat space limit  $f = l = p = s = 1$ .

The purely magnetic gauge connection has six nonvanishing components and reads

$$\begin{aligned} \mathcal{A} = & \frac{1}{2} u_3 a_r(r, \theta) dr + \frac{1}{2} u_3 a_\theta(r, \theta) d\theta \\ & + \left( \frac{1}{2} u_1 \chi^1(r, \theta) + \frac{1}{2} u_2 \chi^2(r, \theta) + \frac{n}{2} u_3 \right) d\varphi + \left( \frac{1}{2} u_1 \xi^1(r, \theta) + \frac{1}{2} u_2 \xi^2(r, \theta) + \frac{n}{2} u_3 \right) d\psi, \end{aligned} \quad (6)$$

---

<sup>2</sup>The choice of a Chern–Simons term  $\varepsilon_{\lambda\mu\nu\rho\sigma} \text{Tr} A_\lambda (F_{\mu\nu} F_{\rho\sigma} - F_{\mu\nu} A_\rho A_\sigma + \frac{2}{5} A_\mu A_\nu A_\rho A_\sigma)$  scaling as  $L^{-5}$  is a possibility, albeit a considerably harder problem technically, and is at present under active consideration.

where  $u_1 = \sin n(\varphi + \psi)\sigma_1 - \cos n(\varphi + \psi)\sigma_2$ ,  $u_2 = \cos n(\varphi + \psi)\sigma_1 + \sin n(\varphi + \psi)\sigma_2$ ,  $u_3 = \sigma_3$ ,  $\sigma_i$  being the Pauli matrices and  $n$  the winding number of the solutions,  $n = 1, 2, \dots$ . In the flat space limit, the reduced action density describes a  $U(1)$  Higgs like model with two effective Higgs fields  $\chi^A$  and  $\xi^A$  ( $A = 1, 2$ ), coupled minimally to the  $U(1)$  gauge connection  $(a_r, a_\theta)$  [31]:

$$\begin{aligned} L_1 &= \frac{\tau_1}{4} \left[ \rho\sigma f_{\rho\sigma}^2 + \frac{\rho}{\sigma} (|\mathcal{D}_\rho\chi^A|^2 + |\mathcal{D}_\sigma\chi^A|^2) + \frac{\sigma}{\rho} (|\mathcal{D}_\rho\xi^A|^2 + |\mathcal{D}_\sigma\xi^A|^2) + \frac{1}{\rho\sigma} (\varepsilon^{AB}\chi^A\xi^B)^2 \right], \\ L_2 &= \frac{\tau_2}{12\rho\sigma} (\varepsilon_{AB}\chi^A\xi^B f_{\rho\sigma} + \mathcal{D}_{[\rho}\chi^A\mathcal{D}_{\sigma]}\xi^A)^2. \end{aligned} \quad (7)$$

Here the Abelian curvature is defined as

$$f_{\rho\sigma} = \partial_\rho a_\sigma - \partial_\sigma a_\rho \quad (8)$$

and the covariant derivatives of the scalar fields are

$$\begin{aligned} \mathcal{D}_\rho\chi^A &= \partial_\rho\chi^A + a_\rho(\varepsilon\chi)^A, & \mathcal{D}_\sigma\chi^A &= \partial_\sigma\chi^A + a_\sigma(\varepsilon\chi)^A, \\ \mathcal{D}_\rho\xi^A &= \partial_\rho\xi^A + a_\rho(\varepsilon\xi)^A, & \mathcal{D}_\sigma\xi^A &= \partial_\sigma\xi^A + a_\sigma(\varepsilon\xi)^A. \end{aligned} \quad (9)$$

The total mass-energy  $M$  of the system is

$$M = \int d^4x \sqrt{g} \mathcal{L}_m = \int_0^\infty dr \int_0^{\pi/2} d\theta \left[ \frac{1}{2} r^3 \sin\theta \cos\theta (\phi_{,r}^2 + \frac{1}{r^2} \phi_{,\theta}^2) + (e^{2a\phi} L_1 + e^{6a\phi} L_2) \right], \quad (10)$$

and equals the total action of solutions, viewed as solitons in a  $d = 4$  Euclidean space.

## 1.2 Topological charge

In our normalisation, the topological charge is defined as

$$q = \frac{1}{32\pi^2} \varepsilon_{\mu\nu\rho\sigma} \int \text{Tr}\{\mathcal{F}_{\mu\nu}\mathcal{F}_{\rho\sigma}\} d^4x, \quad (11)$$

which after integration of the azimuthal angles  $(\varphi_1, \varphi_2)$  reduces to

$$q = \frac{1}{2} \varepsilon_{\mu\nu} \int \left( \frac{1}{2} \varepsilon_{AB}\chi^A\xi^B f_{\mu\nu} + \mathcal{D}_\mu\chi^A\mathcal{D}_\nu\xi^A \right) d^2x \quad (12)$$

$$= \frac{1}{4} \int \varepsilon_{\mu\nu} \partial_\mu (\chi^A\mathcal{D}_\nu\xi^A - \xi^A\mathcal{D}_\nu\chi^A) d^2x. \quad (13)$$

The integration in (12) is carried out over the 2 dimensional space  $x_\mu = (x_\rho, x_\sigma)$ . As expected this is a total divergence expressed by (13).

Using Stokes' theorem, the two dimensional integral of (13) reduces to the one dimensional line integral

$$q = \frac{1}{4} \int \chi^A \overleftrightarrow{\mathcal{D}}_\mu \xi^A ds_\mu, \quad (14)$$

This integral has been evaluated in [31] by reading off the appropriate values of  $\chi^A$  and  $\xi^A$  from the boundary conditions we impose. The result is

$$q = \frac{1}{2} [1 - (-1)^m] n_1 n_2. \quad (15)$$

### 1.3 Numerical results

Apart from the coupling constants  $\tau_1$  and  $\tau_2$  the model contains also the dilaton constant  $a$ . Dimensionless quantities are obtained by rescaling

$$\phi \rightarrow \phi/a, \quad r \rightarrow r(\tau_2/\tau_1)^{1/4}, \quad (16)$$

This reveals the existence of one fundamental parameter which gives the strength of the dilaton-nonabelian interaction

$$\alpha^2 = a^2 \tau_1^{3/2} / \tau_2^{1/2}, \quad (17)$$

which is a feature present also in the EYM case [10].

One can see that the limit  $\alpha \rightarrow 0$  can be approached in two ways and two different branches of solutions may exist. The first limit corresponds to a pure  $p = 1$  YM theory with vanishing dilaton and  $p = 2$  YM terms, the solutions here replicating the (multi-)instantons and composite instanton-antiinstanton bound states discussed in [31]. The other possibility corresponds to a finite value of the dilaton coupling  $a$  as  $\tau_1 \rightarrow 0$ . Thus, the second limiting configuration is a solution of the truncated  $p = 2$  YM system interacting with the dilaton, with no  $p = 1$  YM term. We have studied YMd solutions with  $m = 1, 2$ . From our knowledge of the topological charges (15), the  $m = 1$  solutions will describe (multi)solitons and the  $m = 2$  solutions, soliton-antisoliton configurations. Also, to simplify the general picture we set  $n_1 = n_2 = n$ .

The spherically symmetric solutions are found by using a standard differential equations solver. The numerical calculations in the bi-azimuthally symmetric case were performed with the software package CADSOL, based on the Newton-Raphson method [33].

It turns out that  $m = 1$  solutions with all  $n$  and  $m = 2$  solutions with  $n = 1$  exist for a range of  $\alpha$  starting from a  $\alpha \rightarrow 0$  limit, but do not persist all the way up to the second  $\alpha \rightarrow 0$  limit. (However, the way the solutions approach the limit  $\alpha \rightarrow 0$  depends on  $m$ .) By contrast we find that  $m = 2$  solutions with all  $n > 1$ , exist for all  $\alpha$  between the two limits.

#### $m = 1, n = 1$ : spherically symmetric solutions

The picture we found is very similar to that found for the EYM system [10], the dilaton coupling constant playing the role of the Newton constant. First, for a given  $\alpha$ , solutions with the right asymptotics exist for a single value of the "shooting" parameter. For  $\alpha$  small enough, a branch of solutions smoothly emerges from the BPST configuration [44]. When  $\alpha$  increases, the mass  $M$  and the absolute value of the dilaton function at the origin increase. These solutions exist up to a maximal value  $\alpha_{max} \simeq 0.36928$  of the parameter  $\alpha$ .

As in the corresponding gravitating case [10], we found another branch of solutions in the interval  $\alpha \in [\alpha_{cr(1)}, \alpha_{max}]$  with  $\alpha_{cr(1)}^2 \simeq 0.2653$ . On this second branch of solutions, both  $\phi(0)$  and  $M$  continue to increase but stay finite. However, a third branch of solutions exists for  $\alpha \in [0.2653, 0.2652]$ , on which the two quantities increase further. A fourth branch of solutions has also been found, with a corresponding  $\alpha_{cr(3)} \simeq 0.2642$ . The mass  $M$ , the value of the dilaton field at the origin  $\phi(0)$  and the initial (shooting) parameter  $b$  increase along these branches. Further branches of solutions, exhibiting more oscillations around  $\alpha \simeq 0.264$  are very likely to exist but their study is a difficult numerical problem. This critical behaviour is described as a *conical fixed point* in the analytic analysis in [12]. Therefore we conclude that, as in the spherically symmetric gravitating case [10], the limit  $\tau_1 = 0$  is not approached for solutions with  $m = 1, n = 1$ .

#### $m = 1, n > 1$ : multisoliton solutions with biaximuthal symmetry

These solutions are constructed by starting with the known spherically symmetric configuration and increasing the winding number  $n$  in small steps. The iterations converge, and repeating

the procedure one obtains in this way solutions for arbitrary  $n$ . The physical values of  $n$  are integers.

Any spherically symmetric configuration appears to result in generalisations with higher winding numbers  $n$ . Moreover, the branch structure noticed for the  $m = 1, n = 1$  case seems to be retained by the higher winding number  $m = 1$  solutions. Again, the first branch of solutions exists up to a maximal value of  $\alpha$ , where another branch emerges, extending backwards in  $\alpha$ . We managed to construct higher winding number  $n$  counterparts of the first two branches of spherically symmetric solutions. The mass  $M$  and the absolute value of the dilaton function at the origin increase along these branches.

The functions  $a_\theta$  and  $\phi$  have a small  $\theta$  dependence (although the angular dependence increases with  $n$ ), while  $\chi_1$  and  $\xi_1$  have rather similar shapes. The action density  $\mathcal{L}$  possesses one maximum on the  $\theta = \pi/4$  hyperplane. All multicharge solutions found have concentrated energy and charge density profiles where individual (unit) charge constituents do not appear as distinct components. The moduli of the effective Higgs fields  $|\chi| = (\chi^A \chi^A)^{1/2}$  and  $|\xi| = (\xi^A \xi^A)^{1/2}$  possess one node each on the  $\rho$  and the  $\sigma$  axes, respectively, which coincide with the maximum of the action density. The position of this node moves inward along the first and second branches.

### 1.3.1 $m = 2, n = 1$ configurations: soliton-antisoliton pairs

The  $m = 2$  configurations can be thought of as composite systems consisting of two components which are pseudoparticles of topological charges  $\pm n$ . Thus, these configurations reside in the topologically trivial sector and carry no Chern-Pontryagin topological charge. This type of solutions have no spherically symmetric limit. Also, their behaviour as a function of  $\alpha$  is different from those with  $m = 1$  presented above, in that solutions for all values of  $\alpha$  exist between the two distinct limits of  $\alpha \rightarrow 0$  implied by (17), for all  $n$  except for  $n = 1$ .

It is perhaps interesting to note from the outset that  $m = 2, n = 1$  solutions to be described now, have apparently no counterpart in the  $4 + 0$  dimensional  $p = 1$  YM model studied in [31]. (It turns out that for the  $(m = 2, n = 1)$  solution in that case there is no analytic proof of existence either.) The obvious difference of the  $4 + 1$  dimensional model (1) here and the  $4 + 0$  dimensional  $p = 1$  YM model is that the solutions of the former are parametrised by the effective coupling constant  $\alpha$ , while the latter has no such parameter. As will be described below,  $m = 2, n = 1$  solutions exist for a certain range of  $\alpha$ , and this range excludes the limiting case where the contribution to the action of the dilaton term and the  $p = 2$  YM term in (1) disappear, *i.e.* a  $\mathcal{F}_{MN}^2$  model.

We find that in the limit  $\alpha \rightarrow 0$  resulting from  $a \rightarrow 0$ , *cf.* (17), no solutions of this type exist. However in the limit  $\alpha \rightarrow 0$  corresponding to a finite value of the dilaton coupling  $a$  as  $\tau_1 \rightarrow 0$ , such solutions exist. This limiting configuration is then a solution of the truncated system consisting of the dilaton term and  $p = 2$  YM term  $\mathcal{F}_{MNR}^2$ , which dominate. Its characteristic feature is that for this configuration both nodes of the effective Higgs fields  $|\chi|$  and  $|\xi|$  merge on the  $\theta = \pi/4$  axis. A family of solutions of the model (1) emerges from this configuration. As  $\alpha$  increases, the nodes move towards the symmetry axes,  $\rho$  and  $\sigma$ , respectively, forming two identical vortex rings whose radii slowly decrease while the separation of both rings from the origin increase. At the critical value  $\alpha_{cr} \simeq 0.265$  the node structure of the configuration changes, both vortex rings shrink to zero size and two isolated nodes appear on each symmetry axis. This structure is known for the usual YM system in  $d = 4 + 0$  [31], indeed, increasing of  $\alpha$  along this branch can be associated with increasing of the coupling  $\tau_1$  w.r.t.  $\tau_2$  as the dilaton coupling  $a$  remains fixed; then the term  $\mathcal{F}_{MN}^2$  becomes leading. The maximum of the action density however is still located on  $\theta = \pi/4$  hyperplane.

Another similarity with the instanton-antiinstanton solution of the  $d = 4 + 0, p = 1$  YM theory is that the gauge functions  $a_r, a_\theta$  as well the dilaton function  $\phi$  of the  $n = 1, m = 2$  solutions also are almost  $\theta$ -independent. Along this branch the mass of the solutions grows with increasing  $\alpha$  since with increasing coupling  $\tau_1$  the contribution of the term  $\mathcal{F}_{MN}^2$  also increases.

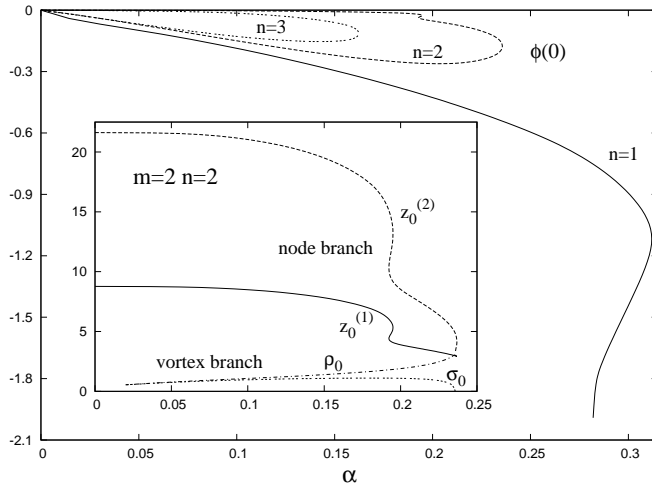


Figure 1: The values of the dilaton function  $\phi$  at the origin of the configuration with  $m = 2$ ,  $n = 1, 2, 3$  are shown as functions of the effective coupling constant  $\alpha$ . The position of nodes ( $z_0^{(1)}$ ,  $z_0^{(2)}$ ) is also presented for  $m = 2$  particle-like solutions with  $n = 1, 2$ .

As the effective coupling increases further beyond  $\alpha_{cr}$  the relative distance between the nodes increases, one lump moving towards the origin while the other one moves in the opposite direction. Along this branch both the value of the dilaton field at the origin  $|\phi(0)|$  and mass of configuration  $M$  increase as  $\alpha$  increases. This branch extends up to a maximal value  $\alpha_{max}^{(1)} \simeq 0.311$  beyond which the dilaton coupling becomes too strong for the static configuration to persist. The second branch, whose energy is higher, extends backwards up to  $\alpha_{max}^{(2)} \simeq 0.279$ . Along this branch both  $|\phi(0)|$  and the mass of the configuration continue to increase as  $\alpha$  decreases. Also the separation between the nodes decreases and both nodes invert direction of the motion, moving toward each other along this branch.

### $m = 2, n = 2$ : double charged solitons-antisoliton pair

This configuration also resides in the topologically trivial sector and can be considered as consisting of two solitons of charges  $n = \pm 2$ . Then the interaction between the nonabelian matter fields becomes stronger than in the case of unit charge constituents and the expected pattern of possible branches of solutions is different from the  $n = 1$  case above.

Indeed, the  $n = 2, m = 2$  solutions show a different dependence on the coupling constant  $\alpha$ , with two branches of solutions. The lower branch emerges from the corresponding solution in pure  $p = 1$  YM theory with vanishing dilaton and  $p = 2$  YM terms, replicating the corresponding solution in [31]. The variation of the effective coupling along this branch is associated with the decrease of  $\tau_1$ , at fixed  $\tau_2$  and fixed dilaton coupling  $a$ . The second branch emerges from a solution of the  $p = 2$  YM-dilaton system, the unrescaled mass  $M$  diverging in this limit, with the rescaled mass  $M\alpha^2$  vanishing. At the maximal value  $\alpha_{max} \simeq 0.2372$  this branch bifurcates with the lower YM branch. For larger values of  $\alpha$ , the dilaton coupling becomes too strong for the static configurations to persist. Thus for  $0 \leq \alpha < \alpha_{max}$  we notice the existence of (at least) two distinct solutions for the same value of coupling constant.

For the same value of  $\alpha$ , the mass of the second branch solution is larger than that of the corresponding lower branch configuration(s). One should also notice the existence of a curious backbending of the lower branch for  $0.193 < \alpha < 0.218$ . Four distinct solutions exist in this case for the same value of  $\alpha$  (three of them located on the lower branch), distinguished by the value of the mass and the dilaton field at the origin.

Again, observation of the positions and structure of the nodes of the effective scalar fields allows us to better understand the behaviour of the solutions. For lower branch solutions with

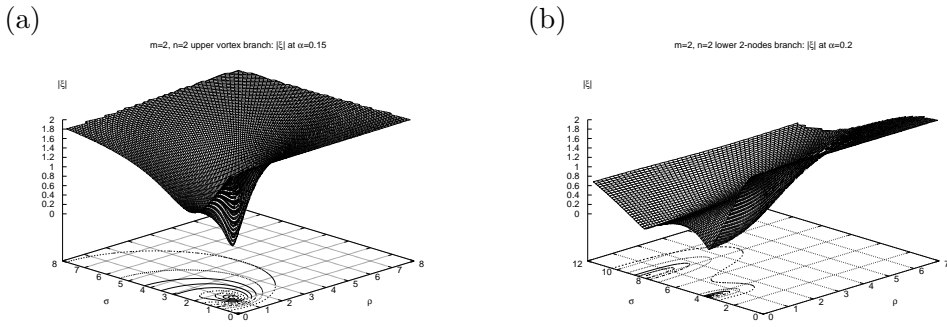


Figure 2: The modulus of the effective Higgs field  $\xi$  is shown for the upper branch  $m = 2, n = 2$  solutions at  $\alpha = 0.15$  (vortex structure, left) and  $\alpha = 0.20$  lower energy branch solution (double node structure, right) as functions of the coordinates  $\rho$  and  $\sigma$ .

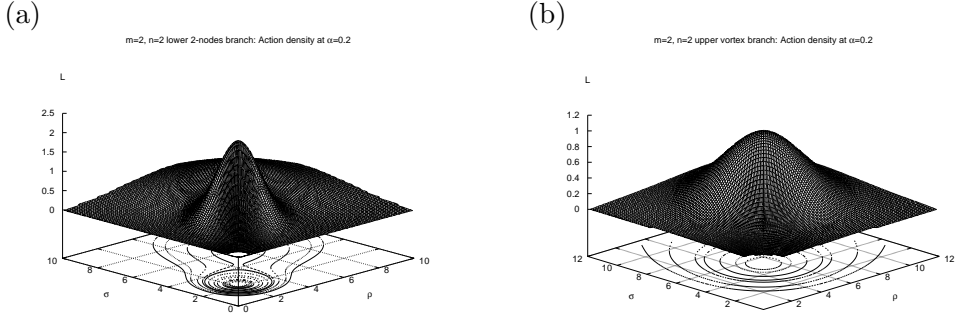


Figure 3: The action density distributions of the  $m = 2, n = 2$  solutions at  $\alpha = 0.20$  are also shown on the lower branch (left) and on the upper branch (right), respectively.

small values of  $\alpha$  there are two (double) nodes of the fields  $|\chi|$  and  $|\xi|$  on the  $\rho$  and  $\sigma$  symmetry axes respectively. The locations of nodes correspond to the locations of the two individual constituents and the action density distribution possesses two distinct maxima on the  $\theta = \pi/4$  axis. The distance between these nodes changes only slightly along the lower mass branch. The backbending in  $\alpha$  observed in this case is reflected also for in the relative positions of the nodes. At the maximal value of  $\alpha$ , the inner node is located at  $\rho_0^{(1)} = \sigma_0^{(1)} \simeq 2.97$  and the outer node is located at  $\rho_0^{(2)} = \sigma_0^{(2)} \simeq 4.18$ .

Along the upper branch, as  $\alpha$  slightly decreases below  $\alpha_{max}$ , the inner node inverts direction of its movement toward the outer node which still moves inwards. Thus, both nodes on the symmetry axis rapidly approach each other and merge forming a two vortex ring solution as  $\alpha \simeq 0.2355$ . The action density then has a single maximum on  $\theta = \pi/4$  axis. As  $\alpha$  decreases further both nodes move away from the symmetry axis and their positions do not coincide with the location of the maximum of the action density. Further decreasing  $\alpha$  results in the increase of the radii of the two rings around the symmetry axis, and in the limit  $\alpha \rightarrow 0$  the rings touch each other on the  $\theta = \pi/4$  axis.

In Figure 1 we give three dimensional plots of the modulus of the effective Higgs field  $\xi$  for the  $n = m = 2$  upper branch vortex solution at  $\alpha = 0.20$  and the  $n = m = 2$  lower branch double node solution at the same value of  $\alpha$ . The action density as given by (1) is also plotted at  $\alpha = 0.20$  both for the upper and for the lower branches.

The numerical calculations indicate the possibility that the solutions of the fundamental YM branch, namely the branch on which the  $p = 1$  YM term dominates, are not unique. It is possible that higher linking number configurations with higher masses might exist.

## 2 $d = 4 + 1$ Einstein-Yang–Mills solitons

We are now in position to extend our discussion of the  $d = 4+1$  YMd system to a gravitating YM system. Our aim is to solve more complex numerical problem of constructing asymptotically flat non-spherically symmetric finite mass EYM solutions. These configurations present a spacetime symmetry group  $R \times U(1) \times U(1)$ , where  $R$  denotes time translation symmetry and the  $U(1)$  factors the rotation symmetry in two orthogonal planes.

While we have restricted to five dimensional EYM solutions for technical reasons, this example is of considerable physical relevance since it enters all  $d = 5$  gauged supergravities as the basic building block and one can expect the basic features of its solutions to be generic. Also special about  $d = 5$  gravitating YM is the particular critical properties of the solutions present in all  $d = 4p + 1$  analysed in [12], and first discovered in [10]. Indeed in the  $d = 5$  YM-dilaton (YMd) system discussed in the previous section, these critical properties were present, providing yet another confirmation that dilaton interactions with YM, mimic [30] those with Einstein gravity.

### 2.1 The ansatz and field equations

We consider the five dimensional  $SU(2)$  EYM action

$$S = \int d^5x \sqrt{-g} \left( \frac{R}{16\pi G} - \mathcal{L}_m \right), \quad (18)$$

where the matter field Lagrangian  $\mathcal{L}_m$  is given by (1). Variation of the action (18) with respect to the metric  $g^{\mu\nu}$  and gauge potential  $A_\mu$  leads to the EYM equations

$$R_{\mu\nu} - \frac{1}{2}g_{\mu\nu}R = 8\pi G (T_{\mu\nu}^{(1)} + T_{\mu\nu}^{(2)}), \quad (19)$$

$$\tau_1 D_\mu \mathcal{F}^{\mu\nu} + \frac{1}{2}\tau_2 \{ \mathcal{F}_{\rho\sigma}, D_\mu \mathcal{F}^{\mu\nu\rho\sigma} \} = 0, \quad (20)$$

where

$$T_{\mu\nu}^{(p)} = \text{Tr} \{ \mathcal{F}(2p)_{\mu\lambda_1\lambda_2\dots\lambda_{2p-1}} \mathcal{F}(2p)_{\nu}{}^{\lambda_1\lambda_2\dots\lambda_{2p-1}} - \frac{1}{4p} g_{\mu\nu} \mathcal{F}(2p)_{\lambda_1\lambda_2\dots\lambda_{2p}} \mathcal{F}(2p)^{\lambda_1\lambda_2\dots\lambda_{2p}} \}, \quad (21)$$

is the energy-momentum tensor for the  $p$ -th YM term in (1),  $p = 1, 2$ .

We consider a  $d = 5$  static metric form (5) parametrized by 4 metric functions.

The mass  $M$  of solutions is the conserved charge associated with the Killing vector  $v = \partial/\partial t$  and can be read from the asymptotic expression of the  $g_{tt}$ -component of the metric tensor

$$-g_{tt} = f = 1 - \frac{8GM}{3\pi r^2} + O\left(\frac{1}{r^4}\right). \quad (22)$$

The mass can also be expressed as an integral [32] over the 3-sphere at spacelike infinity,

$$M = \frac{1}{16\pi G} \frac{3}{2} \oint_\infty v^{\mu;\nu} d^3\Sigma_{\mu\nu}. \quad (23)$$

The topological charge of the particle-like solutions as discussed above, is given by (15) (again, for the sake of simplicity we set  $n_1 = n_2 = n$ ):

$$q = \frac{1}{2} [1 - (-1)^m] n^2, \quad (24)$$

Thus, the Pontryagin charge is nonzero only for odd  $m$ , being equal to  $n^2$ . For even values of  $m$ , the solutions will describe soliton-antisoliton bound states.

To evaluate the Hawking temperature and entropy of the black hole solutions, we use the following expansions of the metric functions at the horizon

$$\begin{aligned} f(r, \theta) &= f_2(\theta) \left( \frac{r - r_h}{r_h} \right)^2 + O \left( \frac{r - r_h}{r_h} \right)^3, & p(r, \theta) &= p_2(\theta) \left( \frac{r - r_h}{r_h} \right)^2 + O \left( \frac{r - r_h}{r_h} \right)^3 \\ l(r, \theta) &= l_2(\theta) \left( \frac{r - r_h}{r_h} \right)^2 + O \left( \frac{r - r_h}{r_h} \right)^3 & s(r, \theta) &= s_2(\theta) \left( \frac{r - r_h}{r_h} \right)^2 + O \left( \frac{r - r_h}{r_h} \right)^3. \end{aligned}$$

The zeroth law of black hole physics states that the surface gravity  $\kappa$  is constant at the horizon of the black hole solutions, where  $\kappa^2 = -(1/4)g^{tt}g^{ij}(\partial_i g_{tt})(\partial_j g_{tt})\Big|_{r=r_h}$ . Since from general arguments the Hawking temperature  $T_H$  is proportional to the surface gravity  $\kappa$ ,  $T_H = \kappa/(2\pi)$ , we obtain the relation

$$T_H = \frac{f_2(\theta)}{2\pi r_h \sqrt{s_2(\theta)}}. \quad (25)$$

One can show, with help of the  $(r, \theta)$ -component of the Einstein equations which implies  $f_2 s_{2,\theta} = 2s_2 f_{2,\theta}$ , that the temperature  $T_H$ , as given in (25), is indeed constant.

For the line element (5), the area  $A$  of the event horizon is given by

$$A = 4\pi^2 r_h^3 \int_0^{\pi/2} d\theta \sin \theta \cos \theta \sqrt{\frac{l_2(\theta) p_2(\theta) s_2(\theta)}{f_2^3(\theta)}}. \quad (26)$$

According to the usual thermodynamic arguments, the entropy  $S$  is proportional to the area  $A$ ,  $S = A/4G$ .

We mention here also the Smarr-type relation which follows from (23) together with Einstein equations

$$\frac{2}{3}M = T_H S - \frac{4\pi^2}{6} \int_{r_h}^{\infty} dr \int_0^{\pi/2} d\theta \sin \theta \cos \theta \frac{\sqrt{l p s}}{f} (T_t^t - \frac{1}{3}T). \quad (27)$$

This relation has been used in practice to verify the accuracy of the numerical computation.

## 2.2 Properties of the solutions

For any set of boundary conditions, we have found that the numerical iteration fails to converge for  $\tau_2 = 0$ . Thus, similar to the spherically symmetric case, no reasonable EYM- $p = 1$  solutions with bi-azimuthal symmetry is likely to exist. This agrees with the physical intuition based on a heuristic Derrick-type scaling argument (although a rigorous proof exists for the spherically symmetric limit only [21, 22]). It is the  $p = 2$  YM term, scaling as  $L^{-8}$ , which enables the existence of configurations with finite mass and well defined asymptotics.

As in the spherically symmetric case [10], dimensionless quantities in this model are obtained by rescaling the radial coordinate  $r \rightarrow (\tau_2/\tau_1)^{1/4} r$ . This reveals the existence of one fundamental parameter which gives the strength of the gravitational interaction  $\alpha^2 = \tau_1^{3/2} (16\pi G/\tau_2^{1/2})$ , similar with the parameter of the YMd system (17).

For any set  $(m, n)$ , the limit  $\alpha \rightarrow 0$  can be approached in two ways and two different branches of solutions may exist. The first limit corresponds to a pure  $p = 1$  YM theory in a flat background (*i.e.* no gravity and no  $p = 2$  YM terms), the solutions here replicating the (multi-)instantons and composite instanton-antiinstanton bound states discussed in [31]. The other possibility corresponds to a finite value of  $G$  as  $\tau_1 \rightarrow 0$ . Thus, the second limiting configuration is a solution of the truncated system consisting of  $p = 2$  YM interacting with gravity, with no  $p = 1$  YM term.

### 2.2.1 $m = 1$ configurations

The  $m = 1$  configurations carry a topological charge  $n^2$  and describe (multi-)solitons. The  $n = 1$  spherically symmetric case was discussed in [10] in a Schwarzschild coordinate system. We repeated the numerical analysis of [10] using the isotropic coordinate system (5). In the spherically symmetric limit only two of the functions in (5) are independent,  $f$  and  $s = l = p$ . The dominant term at the gravity decoupling limit  $\alpha \rightarrow 0$  is the  $F(2)$  term, the YM solution being the well known BPST instanton [34]. When  $\alpha$  increases, these solutions get deformed by gravity and the mass  $M$  decreases. At the same time, the values of the metric functions  $f$  and  $s$  at the origin decrease (see Fig 4). This branch of solutions exists up to a maximal value  $\alpha_{\max}$  of the parameter  $\alpha$ . Another branch of solutions is found on the interval  $\alpha \in [\alpha_{cr(1)}, \alpha_{\max}]$ . On this second branch of solutions, both  $f(0)$  and  $s(0)$  continue to decrease but stay finite. However, a third branch of solutions exists for  $\alpha \in [\alpha_{cr(1)}, \alpha_{cr(2)}]$ , on which the two quantities decrease further. A fourth branch of solutions has also been found, with a corresponding  $\alpha_{cr(3)}$  close to  $\alpha_{cr(2)}$ . Along this succession of branches, the values of the metric functions  $f$  and  $s$  at the origin continue to decrease.

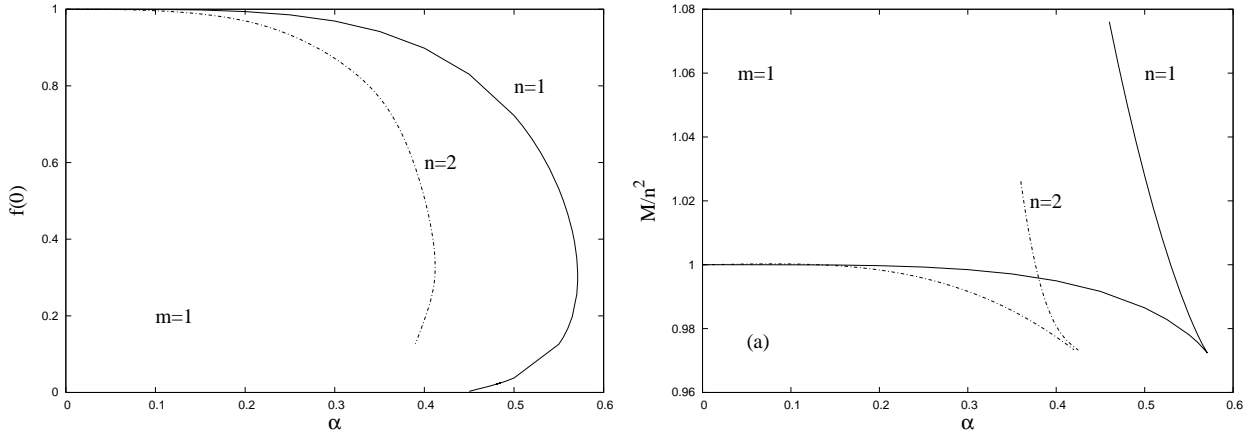


Figure 4: The value at the origin of the metric function  $f$  of the  $m = 1$  particle-like solutions (left) and the mass of the  $m = 1$  particle-like solutions (right) with  $n = 1, 2$  are shown as functions of  $\alpha$ .

On the other hand, the mass parameters do not increase significantly along these secondary branches. This behaviour with respect to the parameter  $\alpha$  is the same as that which was found in [10], for the metric function  $\sigma(r)$  at  $r = 0$ . An analytic explanation of these results was given in [12], where the observed oscillatory behaviour of these functions at  $r = 0$  was characterised as a *conical fixed point*.

The  $n > 1$  non-spherically symmetric solutions are constructed by starting with the known spherically symmetric configuration and increasing the winding number  $n$  in small steps. The iterations converge, and repeating the procedure one obtains in this way solutions for arbitrary  $n$ . The physical values of  $n$  are integers. We have studied  $m = 1$  solutions with  $n = 2, 3$ . As expected, the general features of the spherically symmetric solutions are the same for all  $n > 1$  multi-solitons. Like for the Yang–Mills dilaton (YMd) model discussed in [29], when  $\alpha$  is increased from zero, a branch of gravitating solutions with winding number  $n$  emerges smoothly from the corresponding  $F(2)$  flat space multi-instanton solution.

This branch extends up to a maximal value  $\alpha_{\max}(n)$  of the coupling constant  $\alpha$ , beyond which the numerical iteration fails to converge. The value of  $\alpha_{\max}(n > 1)$  is smaller than the corresponding value in the spherically symmetric case. For example, we find numerically  $\alpha_{\max}(n = 2) \approx 0.412$  while the corresponding value for  $n = 1$  is  $\alpha_{\max} \approx 0.571$ . For all values  $n \geq 1$  we considered, the limiting solutions at  $\alpha_{\max}(n)$  has no special features. A secondary branch, extending backward in  $\alpha$  emerges at  $\alpha_{\max}(n)$ . However, the numerical accuracy deteriorates drastically for the secondary branch of solutions around some critical value  $\alpha_{cr} \sim 0.38$ . Our

numerical results in this case are less conclusive, the properties of these configurations requiring further work. We notice, however, that the value at the origin of all metric functions decreases along these branches, as seen in Figure 4<sup>3</sup>. We expect that the oscillatory pattern of  $g_{tt}(0)$  arising from the *conical fixed point* observed for the spherically symmetric  $m = 1$ ,  $n = 1$  solutions, will also be discovered for the  $n > 1$  solutions here. However, the construction of the secondary branches of solutions is a difficult numerical problem beyond the scope of the present work.

In all cases we have studied, the metric functions  $f$ ,  $l$ ,  $p$ ,  $s$  are completely regular and show no sign of an apparent horizon, while  $l$  and  $p$  have rather similar shapes. The angular dependence of the metric functions is rather small, although it increases somewhat with  $n$ . The gauge functions  $a_r, a_\theta, \chi^A, \xi^A$  look very similar to those of the YMd solutions presented above. Both  $|\chi| = ((\chi^1)^2 + (\chi^2)^2)^{1/2}$  and  $|\xi| = ((\xi^1)^2 + (\xi^2)^2)^{1/2}$  possess one node on the  $\theta = 0$  and  $\theta = \pi/2$  axis, respectively. The positions of these nodes move inward along the branches.

It is also interesting to note that for the  $m = 1$  solutions, the mass per unit charge of the gravitating multisoliton solutions is lower than the mass of a single particle. Thus these multisolitons are gravitationally bound states. This case resembles the situation found for  $d = 4$  gravitating EYMH monopoles with a vanishing or small Higgs selfcoupling [35].

### 2.2.2 $m = 2$ configurations

The  $m = 2$  configurations reside in the topologically trivial sector. These solutions can be thought of as composite systems consisting of two components which are pseudoparticles of Chern-Pontryagin topological charges  $\pm n^2$ . This type of solutions have no spherically symmetric limit. The position of each constituent can be identified according to the location of the maxima of the energy density. Also, the structure and location of the nodes of the (effective Higgs) scalar fields nicely reveal the evolution and the types of the solutions present at the respective values of the gravitational strength.

As in the case of the  $m = 1$  configurations, coupling with gravity yields various branches of gravitating solutions which, however, have different limits depending on the values of the topological charge  $n^2$  of the constituents. Also, their behaviours as functions of the gravitational coupling  $\alpha$  differ from those with  $m = 1$  presented above.

$n = 1$

There is a certain similarity between the properties of the 4+1 dimensional YMd model discussed above [29], and the EYM model under consideration here.

As in the former case, we find that in the limit  $\alpha \rightarrow 0$  resulting from  $G \rightarrow 0$ , no solution with  $n = 1$  exists, *i.e.* that in the gravity decoupling limit no such solution exists. On the other hand, we know from the work of [10] that in the flat space limit the EYM solution of this model reduces to the BPST instanton [34] of the  $p = 1$  (usual) YM model, so that in this limit the  $p = 1$  YM term dominates over the  $p = 2$  term. Thus the nonexistence of a  $m = 2$ ,  $n = 1$  solution here in the gravity decoupling limit implies that there should exist no such solution in the 4 + 0 dimensional  $p = 1$  YM model on flat space. This is precisely what was found in [31].

In the other limit of  $\alpha \rightarrow 0$  however, when both  $\tau_1 \rightarrow 0$  and the gravitational coupling  $G$  remain finite, such solutions exist. It turns out that in this limit, it is the  $p = 2$  term which dominates over the  $p = 1$  YM term. The characteristic feature of this this configuration is that both nodes of the effective Higgs fields  $|\chi|$  and  $|\xi|$  merge on the  $\theta = \pi/4$  hypersurface. From this limiting configuration, a branch evolves as  $\alpha$  increases. Along this branch the nodes move towards the symmetry axes,  $\rho$  and  $\sigma$ , respectively (with  $\rho = r \sin \theta$ ,  $\sigma = r \cos \theta$ ), forming two

---

<sup>3</sup>Note that the values at the origin of all metric functions exhibited in this paper correspond to  $f(r = 0, \theta = 0)$ ,  $s(r = 0, \theta = 0)$ . This restriction is reasonable since for all solutions with bi-azimuthal symmetry that we have found, the metric functions at  $r = 0$  present almost no dependence on the angle  $\theta$ .

identical vortex rings whose radii slowly decrease, while the separation of both rings from the origin also decreases. The evolution of the solution along this branch can be associated with the increase of the coupling  $\tau_1$ , while  $\tau_2$  and the gravitational coupling  $G$  remain fixed. This reproduces the corresponding pattern in the YMd system [29]. Note that there is a difference between the evolutions of the configurations we are considering here in this 4 + 1 dimensional theory, and the behaviour of the gravitating multimonoles or the monopole-antimonopole solutions of the gravitating YMH system 3 + 1 theory [35, 36]. Although the latter also feature different branches, the evolution along those branches is usually associated with the increasing of the gravitational coupling  $G$  on the lower mass branch, and, the decreasing of the VEV of the Higgs field on the upper mass branch. More importantly, the  $m = 2$ ,  $n = 1$  solution in that case does have a gravity decoupling limit. Thus, the gravitating solutions of the 3 + 1 YMH

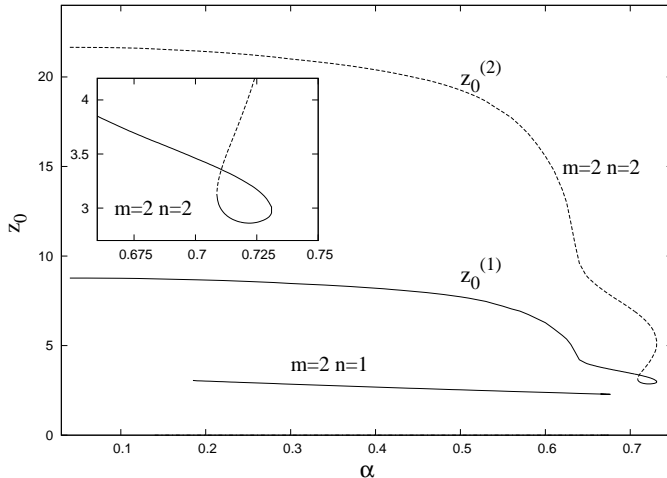


Figure 5: The position of nodes  $(z_0^{(1)}, z_0^{(2)})$  is presented for  $m = 2$  particle-like solutions with  $n = 1, 2$ .

theory usually are linked to flat space configurations, while the solutions discussed here clearly do not have a flat space limit.

On the  $p = 2$  branch (where the  $p = 2$  term  $\mathcal{F}_{MNR}^2$  dominates) of five dimensional EYM  $m = 2$ ,  $n = 1$  solutions, the gauge functions  $a_r$ ,  $a_\theta$  as well the metric functions  $f$  and  $s$  are almost  $\theta$ -independent, whereas the metric functions  $l$  and  $p$  possess reflection symmetry with respect to  $\theta = \pi/4$  axis. The mass of the gravitating solutions on this branch decreases, as well as the values at the origin of the metric functions. At the critical value  $\alpha \simeq 0.672$ , the node structure of the configuration changes and both vortex rings shrink to zero size, two isolated nodes appearing on each symmetry axis. This transition means that the  $p = 1$  term  $\mathcal{F}_{MN}^2$  becomes dominant. This secondary branch has a small extension in  $\alpha$  up to the maximal value  $\alpha_{max} \simeq 0.6765$ , beyond which we could not find regular gravitating solutions. We found instead that this branch merges here with the second,  $p = 1$  branch, which evolves backwards in  $\alpha$  as the value of the metric function  $f(0)$  continues to decrease.

The evolution along this short branch can be associated with the decrease of the coupling constant  $\tau_2$  relative to  $\tau_1$ , as the gravitational coupling  $G$  remains fixed. For this branch the relative distance between the nodes increases, one lump slowly moving towards the origin and the other one moving in the opposite direction. This branch persists up to a value of the coupling constant  $\alpha_{cr} \simeq 0.6665$ , where a critical solution is approached. Due to severe numerical difficulties encountered here, we could not clarify the properties of this critical solution further. As  $\alpha \rightarrow \alpha_{cr}$ , the metric function  $f(0)$  takes a very small value,  $f(0) \simeq 10^{-3}$ , while  $s(0)$  remains one order of magnitude larger. At the same time, the Lagrangian density and the mass of the configuration remain finite at that point. The critical behaviour observed here resembles the case of the gravitating 4+1 EYM vortices in the model consisting only of the  $p = 1$  YM term [21].

It is tempting to speculate that, similar to case in [21], the solution splits into two parts: a non-singular interior region with a special geometry (so-called throat) and an exterior asymptotically flat region where two pseudoparticles are located. However, another parametrisation of the metric, differing from (5) (and possibly even a different numerical approach) appears to be necessary to clarify these aspects.

$$n = 2$$

This configuration also resides in the topologically trivial sector and can be considered as consisting of two pseudoparticles of charges  $\pm 2^2$ . In this case the interaction between the non Abelian matter fields becomes stronger than in the case of  $\pm 1$  constituents, resulting in a different pattern of possible branches of solutions. Indeed, as in the case of the 4+1 dimensional YMd system [29], we observe two different branches of gravitating solutions, both linked to the  $\alpha \rightarrow 0$  limit. The lower branch, on which the  $p = 1$  YM term dominates, emerges from the corresponding flat space solution of the pure YM theory with vanishing  $p = 2$  term. Varying  $\alpha$  along this branch is associated with the decrease of  $\tau_1$ , at fixed  $\tau_2$  and fixed gravitational coupling  $G$ .

For small values of  $\alpha$  the corresponding  $m = 2, n = 2$  solutions possess two (double) nodes of the fields  $|\chi|$  and  $|\xi|$  on the  $\rho$  and  $\sigma$  symmetry axes, respectively. The locations of nodes correspond to the locations of the two individual constituents and the action density distribution possesses two distinct maxima on the  $\theta = \pi/4$  axis. As  $\alpha$  increases the mass of the solution increases and both pseudoparticles move from spatial infinity towards the origin. For values of  $\alpha$  smaller than  $\alpha_{cr} \simeq 0.635$  along this branch, the energy of interaction between the individual pseudoparticles is relatively small and both constituents remain individual. We observe that, as the coupling constant approaches this critical value from below, the energy of interaction rapidly increases and both pseudoparticles form a bound state. This branch extends further up to a maximal value  $\alpha_{max} \simeq 0.7265$  where it bifurcates with an upper  $p = 2$  branch which extends all the way back to  $\alpha = 0$ . Varying  $\alpha$  along this branch is associated with the increase of  $\tau_2$  relative to  $\tau_1$ , as gravitational constant  $G$  remains fixed.

Along the upper branch, as  $\alpha$  slightly decreases below  $\alpha_{max}$ , the inner node inverts direction of its movement toward the outer node which still moves inwards. Thus, both nodes on the symmetry axis rapidly approach each other and merge forming a two vortex ring solution at  $\alpha \simeq 0.708$ . The action density then has a single maximum on  $\theta = \pi/4$  axis. As  $\alpha$  decreases further both nodes move away from the symmetry axis and their positions do not coincide with the location of the maximum of the action density. Further decreasing  $\alpha$  results in the increase of the radii of the two rings around the symmetry axis, and in the limit  $\alpha \rightarrow 0$  the rings touch each other on the  $\theta = \pi/4$  hyperplane.

### 2.3 Black hole solutions

According to the standard arguments, one can expect black hole generalisations of the regular configurations to exist at least for small values of the horizon radius  $r_h$ . This is confirmed by the numerical analysis for  $m = 1, n = 2$ . Several black hole solutions with  $m = 2, n = 1$  have been also constructed, with a lower numerical accuracy, however. As discussed in [10] spherically symmetric  $m = 1, n = 1$  black hole counterparts exist for any regular solution with the same amount of symmetry. Starting for a given  $\alpha_0 < \alpha_{max}$  from a  $r_h = 0$  first branch regular solution, one finds a branch of black hole solutions extending up to a maximal value of the event horizon radius  $r_h = r_h^{max}$ . When  $r_h$  increases, both the mass and the Hawking temperature increase. The value of  $r_{h(max)}$  depends on  $\alpha$ . The Hawking temperature decreases on this branch, while the mass parameter increases; however, the variation of mass is relatively small. The corresponding picture for secondary branches is more complicated and will not be discussed here.

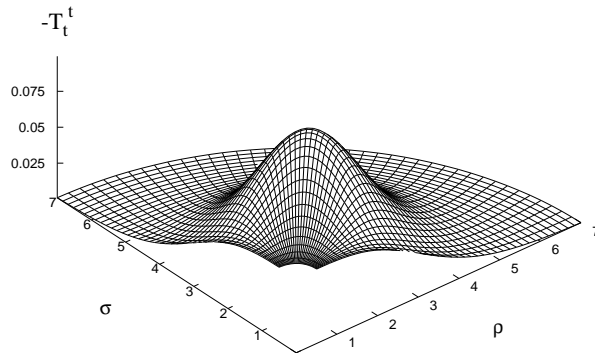


Figure 6: The energy density  $\epsilon = -T_t^t$  is shown as a function of the coordinates  $\rho = r \sin \theta$ ,  $\sigma = \rho \cos \theta$  for a  $m = 1$ ,  $n = 2$  EYM black hole solutions with  $\alpha = 0.2$ ,  $r_h = 0.5$ .

The numerical construction of nonspherically symmetric black hole solutions appears to be more difficult than in the globally regular case. However, our numerical results indicate that the  $m = 1$ ,  $n > 1$  black hole solutions with bi-azimuthal symmetry follow this general pattern. First, black hole solutions seem to exist for all values of  $\alpha$  or which regular configurations could be constructed (here we restrict again to first branch solutions). Also, it appears that black hole solutions exist only for a limited region of the  $(r_h, \alpha)$  space. However, for a given value of  $\alpha$ , it is very difficult to find an accurate value of  $r_h^{\max}$ . An approach to this problem with a different method appears to be necessary.

These solutions possess a regular deformed  $S^3$  horizon. The energy density has a pronounced angle-dependence, with a maximum on the  $\theta = \pi/2$  hypersurface. Figure 5 shows a three dimensional plot of the energy density of a  $m = 1$ ,  $n = 2$  black hole with  $\alpha = 0.2$ ,  $r_h = 0.5$  as a function of the coordinates  $\rho = r \sin \theta$ ,  $\sigma = r \cos \theta$ . With increasing the winding number  $n$ , the absolute maximum of the energy density residing on the  $\rho = \sigma$  axis, shifts inward. The metric and gauge functions possess a nontrivial angular dependence at the horizon.

Outside their event horizon, these black holes possess nontrivial non Abelian fields. Therefore they represent a further counterexample to the  $d = 5$  no-hair conjecture. Also, these bi-azimuthally symmetric black holes clearly show that the higher dimensional static black hole solutions need not be spherically symmetric.

### 3 Conclusions

Motivated by the recent interest in gravitating solutions in higher dimensional spacetime, we have studied static, bi-azimuthally symmetric solutions with non Abelian fields in  $d = 4 + 1$  spacetime dimensions. Our solutions are akin to the static, axially symmetric EYM configurations in  $d = 4$ , studied exhaustively in [37], [38, 39]. Our choice of bi-azimuthal symmetry is motivated by our desire to reduce the boundary value problem to a two dimensional one. An alternative symmetry imposition resulting in a two dimensional residual system would be imposition of  $SO(3)$  spherical symmetry in the 3 dimensional spacelike dimensions like in [28]. We have eschewed this alternative for purely technical reasons (see footnote <sup>1</sup>).

The regular and black hole solutions presented are natural generalisations of the known [10]  $d = 5$  EYM spherically symmetric globally regular and black hole solutions. Like the former they are asymptotically flat, finite mass solutions, that describe nontrivial gravitating magnetic gauge field configurations. Our  $d = 5$  EYM configurations are the first  $d \geq 5$  dimensional static

solutions in the literature, which are not spherically symmetric.

In the case of particle like solutions, which we have studied much more intensively than their black hole counterparts, their dependence on the effective gravity coupling  $\alpha$  is analysed numerically in some detail. By and large this is qualitatively very similar to that for the YMd solutions [29] in  $4 + 1$  dimensions, except that here we have four metric functions to keep track of, as opposed to the single dilaton field in the previous case [29]. We have studied regular solutions with  $m = 2, n = 1$  and  $m = 2, n = 2$  in detail, numerically.

Just as in the YMd case, here too there exists a  $m = 2, n = 1$  solution on the branch where the  $p = 2$  YM term dominates, while on the other branch, where the  $p = 1$  YM term dominates, such a solution is absent. As it turns out the  $p = 1$  YM term dominates in the gravity decoupling limit, which is consistent with our knowledge that this model in  $4 + 0$  dimensions does not support [31] a  $m = 2, n = 1$  solution.

Another qualitative feature of 5 dimensional EYM solutions that is confirmed here is the occurrence of a *conical* singular behaviour with respect to the dependence of the metric functions on  $\alpha$ . This features the oscillatory picture first discovered for the  $m = 1, n = 1$  spherically symmetric solutions in [10] and analysed in [12], which are found also here for the  $m = 1, n > 1$  case.

As compared to the  $d = 4$  case [38, 39], we expect the existence of a much richer set of nonspherically symmetric EYM solutions in  $d = 5$ . The configurations studied here represent only the simplest, asymptotically flat type of  $d = 5$  nonspherically symmetric gravitating non-abelian solutions. For example, it is known that  $d = 5$  Einstein gravity coupled to Abelian fields presents black ring [40] solutions. These solutions have an horizon topology  $S^2 \times S^1$  and approach at infinity the flat  $\mathcal{M}^5$  background, as is the case with our solutions. It would be interesting to construct non Abelian versions of the  $U(1)$  black ring solutions. A black ring can be constructed in a heuristic way by taking a black string, bending the extra dimension and spinning it along the circle direction just enough so that the gravitational attraction is balanced by the centrifugal force. In this framework the (putative) nonabelian black ring would behave locally as a boosted black string, e.g. that in [26], with very similar charges and fields. The numerical work involved in the construction of non spherically symmetric higher dimensional EYM solutions is, however, a considerably challenging task.

## Acknowledgements

We thank Mikhail Volkov for helpful comments and discussions. This work was carried out in the framework of Science Foundation Ireland (SFI) Research Frontiers Programme (RFP) project RFP07/FPHY330. Ya.S. would like to thank the organisers of the Quarks-2008 Seminar for invitation and the hospitality in Sergiev Posad.

## References

- [1] M. S. Volkov and D. V. Gal'tsov, Phys. Rept. **319** (1999) 1 [arXiv:hep-th/9810070].
- [2] M. S. Volkov, arXiv:hep-th/0612219.
- [3] F. R. Tangherlini, Nuovo Cim. **27** (1963) 636.
- [4] R. C. Myers and M. J. Perry, Annals Phys. **172** (1986) 304.
- [5] R. Emparan and H. S. Reall, Phys. Rev. Lett. **88** (2002) 101101 [arXiv:hep-th/0110260].
- [6] H. Elvang and P. Figueras, arXiv:hep-th/0701035.
- [7] G. T. Horowitz and A. Strominger, Nucl. Phys. B **360** (1991) 197.
- [8] R. Bartnik and J. McKinnon, Phys. Rev. Lett. **61** (1988) 141.

- [9] Y. Brihaye, A. Chakrabarti and D. H. Tchrakian, *Class. Quant. Grav.* **20** (2003) 2765 [arXiv:hep-th/0202141].
- [10] Y. Brihaye, A. Chakrabarti, B. Hartmann and D. H. Tchrakian, *Phys. Lett. B* **561** (2003) 161 [arXiv:hep-th/0212288].
- [11] Y. Brihaye, E. Radu and D. H. Tchrakian, *Int. J. Mod. Phys. A* **19** (2004) 5085 [arXiv:hep-th/0405255].
- [12] P. Breitenlohner, D. Maison and D. H. Tchrakian, *Class. Quant. Grav.* **22** (2005) 5201 [arXiv:gr-qc/0508027].
- [13] E. Radu and D. H. Tchrakian, *Phys. Rev. D* **73** (2006) 024006 [arXiv:gr-qc/0508033].
- [14] E. Radu, C. Stelea and D. H. Tchrakian, *Phys. Rev. D* **73** (2006) 084015 [arXiv:gr-qc/0601098].
- [15] Y. Brihaye, E. Radu and D. H. Tchrakian, *Phys. Rev. D* **75** (2007) 024022 [arXiv:gr-qc/0610087].
- [16] D. H. Tchrakian, *Phys. Lett. B* **150** (1985) 360.
- [17] D.H. Tchrakian, *Yang-Mills hierarchy*, in *Differential Geometric Methods in Theoretical Physics*, eds. C.N. Yang, M.L. Ge and X.W. Zhou, *Int. J. Mod. Phys. A (Proc.Suppl.)* **3A** (1993) 584.
- [18] A.A. Tseytlin, *Born-Infeld action, supersymmetry and string theory*, in *Yuri Golfand memorial volume*, ed. M. Shifman, World Scientific (2000).
- [19] E. Bergshoeff, M. de Roo and A. Sevrin, *Fortsch.Phys.* **49** (2001) 433-440; *Nucl.Phys.Proc.Suppl.* **102** (2001) 50-55. E. A. Bergshoeff, M. de Roo and A. Sevrin, *Fortsch. Phys.* **49** (2001) 433 [*Nucl. Phys. Proc. Suppl.* **102** (2001) 50] [arXiv:hep-th/0011264].
- [20] M. Cederwall, B. E. W. Nilsson and D. Tsimpis, *JHEP* **0106** (2001) 034 [arXiv:hep-th/0102009].
- [21] M. S. Volkov, *Phys. Lett. B* **524** (2002) 369 [arXiv:hep-th/0103038].
- [22] N. Okuyama and K. I. Maeda, *Phys. Rev. D* **67** (2003) 104012 [arXiv:gr-qc/0212022].
- [23] P. Breitenlohner, P. Forgacs and D. Maison, *Nucl. Phys.* **B 383** (1992) 357; *ibid.* **442** (1995) 126
- [24] Y. Brihaye, B. Hartmann and E. Radu, *Phys. Rev. D* **71** (2005) 085002 [arXiv:hep-th/0502131].
- [25] B. Hartmann, *Phys. Lett. B* **602** (2004) 231 [arXiv:hep-th/0409006].
- [26] Y. Brihaye, B. Hartmann and E. Radu, *Phys. Rev. D* **72** (2005) 104008 [arXiv:hep-th/0508028].
- [27] Y. Brihaye and E. Radu, *Phys. Lett. B* **641** (2006) 212 [arXiv:hep-th/0606228].
- [28] E. Witten, *Phys. Rev. Lett.* **38** (1977) 121.
- [29] E. Radu, Y. Shnir and D. H. Tchrakian, *Phys. Rev. D* **75** (2007) 045003 [arXiv:hep-th/0611270].

- [30] D. Maison, Commun. Math. Phys. **258** (2005) 657 [arXiv:gr-qc/0405052];  
G. Lavrelashvili and D. Maison, Phys. Lett. B **295** (1992) 67.
- [31] E. Radu and D. H. Tchrakian, Phys. Lett. B **636** (2006) 201 [arXiv:hep-th/0603071].
- [32] A. Komar, Phys. Rev. **113** (1959) 934.
- [33] W. Schönauer and R. Weiß, J. Comput. Appl. Math. **27**, 279 (1989);  
M. Schauder, R. Weiß and W. Schönauer, *The CADSOL Program Package*, Universität Karlsruhe, Interner Bericht Nr. 46/92 (1992);  
W. Schönauer and E. Schnepf, ACM Trans. on Math. Soft. **13**, 333 (1987).
- [34] A. A. Belavin, A. M. Polyakov, A. S. Shvarts and Y. S. Tyupkin, Phys. Lett. B **59** (1975) 85.
- [35] B. Hartmann, B. Kleihaus and J. Kunz, Phys. Rev. D **65**, 024027 (2002) [arXiv:hep-th/0108129];  
B. Hartmann, B. Kleihaus and J. Kunz, Phys. Rev. Lett. **86**, 1422 (2001) [arXiv:hep-th/0009195];  
B. Kleihaus and J. Kunz, Phys. Rev. Lett. **85**, 2430 (2000) [arXiv:hep-th/0006148];  
Y. Brihaye, B. Hartmann and J. Kunz, Phys. Lett. B **441**, 77 (1998) [arXiv:hep-th/9807169].
- [36] B. Kleihaus, J. Kunz and Y. Shnir, Phys. Rev. D **71** (2005) 024013 [arXiv:gr-qc/0411106].
- [37] B. Kleihaus and J. Kunz, Phys. Rev. D **57** (1998) 834 [arXiv:gr-qc/9707045].
- [38] R. Ibadov, B. Kleihaus, J. Kunz and M. Wirschins, Phys. Lett. B **627** (2005) 180 [arXiv:gr-qc/0507110].
- [39] R. Ibadov, B. Kleihaus, J. Kunz and Y. Shnir, Phys. Lett. B **609** (2005) 150 [arXiv:gr-qc/0410091].
- [40] H. Elvang, Phys. Rev. D **68** (2003) 124016 [arXiv:hep-th/0305247];  
R. Emparan, JHEP **0403** (2004) 064 [arXiv:hep-th/0402149].
- [41] M.B. Green, J.H. Schwarz and E. Witten, *Superstring Theory*, Cambridge University Press, Cambridge, 1987.
- [42] M. Cederwall, B. Nilsson and D. Tsimpis, JHEP **0106** (2001) 034.
- [43] C. Rebbi and P. Rossi, Phys. Rev. D **22** (1980) 2010.
- [44] A. A. Belavin, A. M. Polyakov, A. S. Shvarts and Y. S. Tyupkin, Phys. Lett. B **59** (1975) 85.